

HETEROCYCLES, Vol. 77, No. 2, 2009, pp. 1019 - 1035. © The Japan Institute of Heterocyclic Chemistry
Received, 30th July, 2008, Accepted, 30th September, 2008, Published online, 2nd October, 2008
DOI: 10.3987/COM-08-S(F)80

SYNTHESIS AND PROPERTIES OF NOVEL BIOLOGICALLY INTERESTING POLYCYCLIC 1,3,4-OXADIAZOLES CONTAINING ACRIDINE/ACRIDONE MOIETIES[†]

Zdenka Fröhlichová,¹ Jana Tomaščíková,¹ Ján Imrich,^{1,*} Pavol Kristian,¹ Ivan Danihel,¹ Stanislav Böhm,² Danica Sabolová,¹ Mária Kožurková,¹ and Karel D. Klika³

¹ Institute of Chemistry, Faculty of Science, P. J. Šafárik University, SK-041 67 Košice, Slovak Republic. Email: jan.imrich@upjs.sk

² Department of Organic Chemistry, Institute of Chemical Technology, CZ-166 28 Prague, Czech Republic

³ Department of Chemistry, University of Turku, FIN-20014 Turku, Finland

Abstract – A series of polycyclic 1,3,4-oxadiazoles bearing acridine and acridone pharmacophores were synthesized as potential noncovalent DNA-binding and antitumor agents. The synthesis of oxadiazoles with acridone moiety was performed exploring oxidative cyclization of corresponding aldimines *via* bromine and the acridine derivatives by cyclization of acylthiosemicarbazides with mercuric oxide. The spectroscopic properties of the compounds in the case of acridonoxadiazoles showed an efficient binding activity to DNA ($K = 5.3\text{--}9.2 \times 10^4 \text{ M}^{-1}$), whereas the acridine analogues are suitable as biomarkers. The structure of compounds were characterized by spectral methods (UV-vis, IR, ¹H, ¹³C, and 2D NMR) and quantum-chemical calculations (DFT, ZINDO).

INTRODUCTION

A number of papers have appeared recently on the interesting biological properties of various oxadiazole derivatives. Of note, some polysubstituted pyrazoles comprising oxadiazole rings exhibited antitumor activity and were found to be anti-HCV agents.¹ Moreover, attention was paid to oxadiazoles with antimicrobial and anti-inflammatory properties²⁻⁴ and other oxadiazoles were also synthesized and found

[†] Dedicated to Professor Emeritus Keiichiro Fukumoto on the occasion of his 75th birthday.

* The author to whom correspondence should be addressed.

to possess expected biological activities.^{5,6} In addition to these properties, oxadiazoles exhibit antifungal, anticonvulsive, pesticidal, hypotensive, hypoglycemic, diuretic, and other activities.^{5,6} Various methods for the synthesis of 1,3,4-oxadiazoles starting from hydrazides exist, e.g. the reaction of hydrazides with isothiocyanates to provide thiosemicarbazides followed by refluxing with mercuric oxide in absolute ethanol¹ or the oxidative cyclization of sugar hydrazones, derived from acylhydrazides and aldopentoses/aldohexoses, with bromine.⁶ An alternative synthesis of 1,3,4-oxadiazoles from hydrazides is the treatment of acylsemicarbazides with POCl₃,⁷ where the acylsemicarbazides are produced from acylthiosemicarbazides by S→O exchange using mesitylnitrile oxide (MNO). 2,5-Disubstituted-1,3,4-oxadiazoles have also been prepared by microwave-assisted synthesis⁴ and by the thermolysis of geminal diazides.⁸

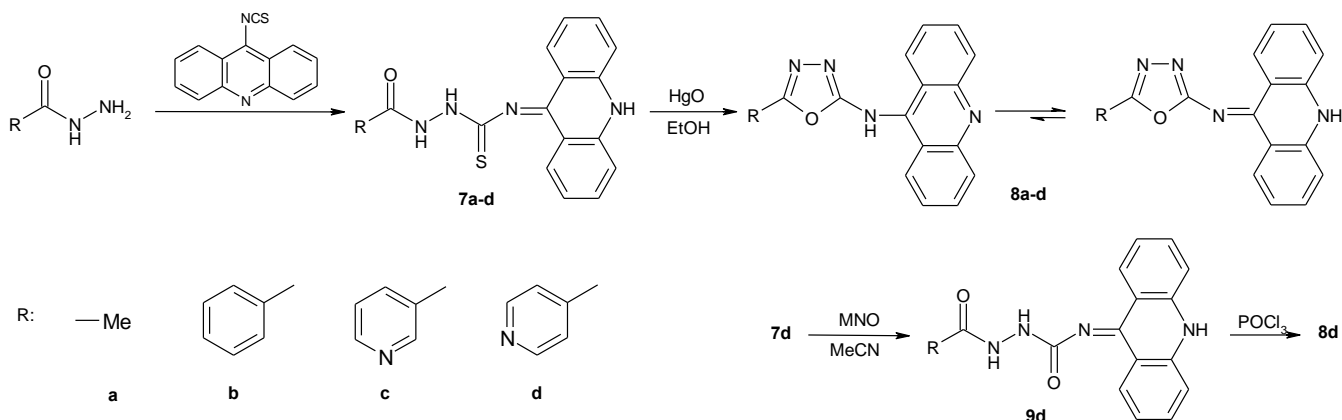
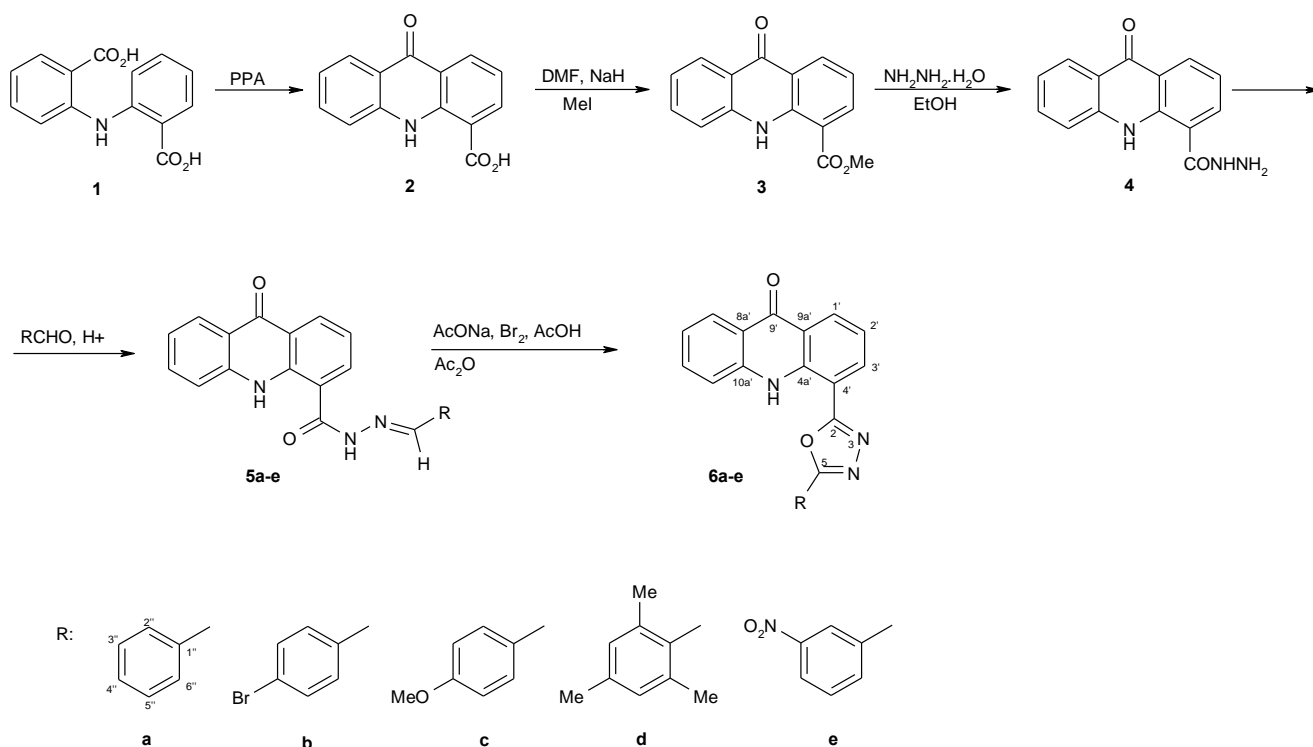
Acridine derivatives are known as excellent intercalating pharmacophores.⁹ The aim of this work was to synthesize and investigate the properties of novel 1,3,4-oxadiazoles substituted with either an acridine or an acridone moiety as part of our continuing interest in biologically active acridine derivatives. The ensuing compounds were characterized spectroscopically using UV-vis, fluorescence, IR, ¹H, ¹³C (2D NMR) and by quantum-chemical calculations using DFT (B3LYP/6-311+G(d,p)) and ZINDO level of theory. Biological activity was evaluated using calf thymus DNA (ctDNA) to ascertain the binding and bio-interaction of the compounds.

RESULTS AND DISCUSSION

Synthesis

The first set of 1,3,4-oxadiazoles containing an acridone moiety was prepared starting from 2,2'-iminodibenzoic acid (**1**) (Scheme 1). Acridonoxadiazoles **6** were obtained from 9-oxo-9,10-dihydro-acridine-4-carboxylic acid **2** synthesized according to method¹⁰ when polyphosphoric acid (PPA) was used for cyclization of **1**. The esterification of **2** to corresponding methyl ester **3** was realized using methyl iodide in DMF/NaH, from which the corresponding hydrazide **4** was prepared by treatment with hydrazine monohydrate. Condensation¹¹ of **4** with a series of aldehydes (RCHO: **a**, R = phenyl; **b**, R = 4-bromophenyl; **c**, R = 4-methoxyphenyl; **d**, R = 2,4,6-trimethylphenyl; **e**, R = 3-nitrophenyl), then yielded aldimines **5a–e**. Aldimines **5a–e** were then cyclized by bromine/acetic acid oxidation⁶ to 1,3,4-oxadiazoles **6a–e**. The second set of 1,3,4-oxadiazoles containing an acridine moiety was then prepared (see Scheme 2) by exploiting acylthiosemicarbazides **7a–d** (acyl groups: **a**, CH₃CO; **b**, PhCO; **c**, 3-pyridinylCO; **d**, 4-pyridinylCO) described in a previous work.^{9b} Compounds **7a–d** were cyclized to 1,3,4-oxadiazoles **8a–d** by refluxing with mercuric oxide in absolute ethanol.¹ For comparative purposes, following better yields, **7d** was also treated with MNO to yield acylsemicarbazide **9d**, which was then cyclized to oxadiazole **8d** using POCl₃.⁷ Comparing the yields of the oxadiazole

products prepared by other methods,¹²⁻¹⁴ this attempt however was not profitable because these were practically the same small (12 and 14%), but the latter was more labor and time consuming. There are two main reasons for the low product yields obtained. The first is that the acridine moiety is not very stable and as well as side reactions leading to decomposition products present in the reaction mixture, also a black-brown precipitant was formed. The second is the very poor solubility of the starting thiosemicarbazides **7a-d** which only formed a suspension in the ethanol.



Spectroscopy and structure

The characteristic ^1H and ^{13}C NMR chemical shifts of the acridone skeleton for oxadiazoles **6a–e** were readily assigned using HSQC and HMBC spectra: the H-10's (ca. 11.5 ppm), C-9's (178 ppm), and the quaternary carbons C-4a' (139 ppm), C-10a' (140 ppm), C-8a' (122 ppm), and C-9a' (122 ppm). The values for these signals are in good agreement with those for the 4-acridone carboxamide imines¹¹ and comparable, except for the carbonyl carbon, with acridine derivatives consisting of a dihydroacridine ring.^{9b} The carbons of the oxadiazole ring resonated at ca. 166 ppm for C-2 and 158 ppm for C-5, which are similar to literature values^{5,15} and which were able to be unambiguously assigned by HMBC correlations from the *ortho* protons of the phenyl substituent. The structures of oxadiazoles **8a–d** possessing an acridine moiety were confirmed to be in the dihydroacridine tautomeric form and this is consistent with expectations as the N-10' atom of the acridinyl moiety is well known^{16,9b,f} for its propensity to retain a proton, i.e. the H-10' tautomer dominates the tautomeric equilibrium depicted in Scheme 2. Characteristic ^1H and ^{13}C NMR chemical shift values, as averaged values for the set, were observed at 118.1 ppm for C-4',5', 140.0 ppm for C-4a',10a', and 12.3 ppm for H-10', though most diagnostic^{16a,b} for the presence of the H-10' tautomer is the shielded position of the C-4',5' signals, in this instance at 118.1 ppm (typically ca. 119 ppm). Uncharacteristically, rotation about the N₁₁–C₉' bond was fast thus rendering the two sides of the acridine moiety equivalent on the NMR timescale in compounds **8a–d**. Though the two sides of the acridine moiety are usually observed as distinct in these compounds, the prevailing conditions can nevertheless increase the rate of exchange to render them equivalent,^{9b} though paradoxically the labile H-10' can still be observed for samples of **8a–d** measured in this work.

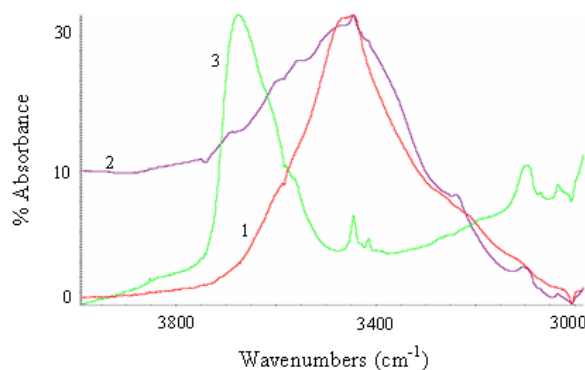


Figure 1. Concentration dependency of the N-H stretching band for **6a** in carbon disulfide. Trace 1: concentration, 1.15 mg/mL; trace 2: diluted 1:10, trace 3: diluted 1:100. Intramolecular vibrations in trace 3: 3414.0 and 3443.2 cm^{-1} .

Taking into account the possibility to form hydrogen bonds in acridone compounds, the concentration dependence of N-H intensity bands in range 3200–3600 cm^{-1} measured in carbon disulfide for derivatives

6a, **6d**, and **6e** was performed (see Experimental). The intensity of the absorption N-H bands with dilution decreased and at dilution 1:100 two new bands occurred (Figure 1) confirming the presence of intramolecular bonding in addition to the intermolecular bonding typical for an acridone skeleton.¹¹ These two bands could be ascribed to N10-H...O(oxadiazole) and N10-H...N (oxadiazole) hydrogen bondings (Figure 1). Two characteristic regions revealed in UV-vis spectra of oxadiazoles **6a–e** and **8a–d**. The first with higher intensity in the region 230–300 nm and the second absorption band (Figure 2) in region at 370–420 nm was registered, which could be attributed to the $\pi \rightarrow \pi^*$ transitions connected with electron transfer due to the conjugation of oxadiazol heterocycles with acridone/acridine skeleton.

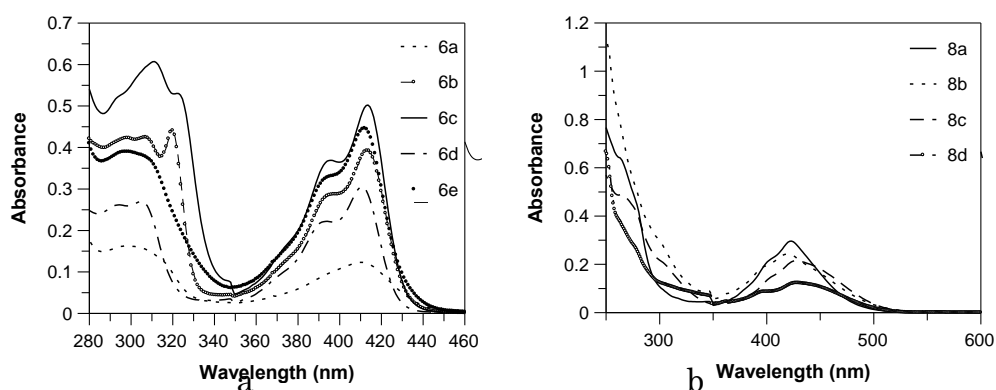


Figure 2. UV-vis spectra of oxadiazoles **6a–e** (a) and **8a–d** (b).

To obtain more details, the semiempirical ZINDO method was used to interpret UV-vis spectra of derivatives **6a** and **8b**. The theoretical and experimental spectra of **6a** are similar but shifted (scaling factor = 1.188). From analysis of electronic transitions followed that all significant transitions are of $\pi \rightarrow \pi^*$ type. The most shifted maximum ($\lambda = 420$ nm, oscillator strength $f = 0.61$) corresponds to HOMO \rightarrow LUMO transition with both two π -orbitals HOMO and LUMO spreading over whole molecular system including phenyl substituent (Figure 3).

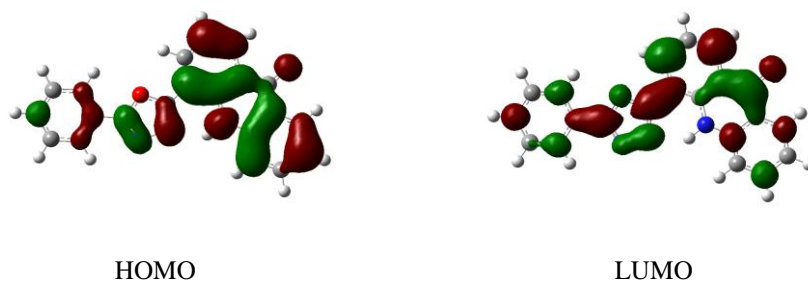


Figure 3. Frontier molecular orbitals HOMO and LUMO for the derivative **6a**.

The situation is similar at HOMO-1 \rightarrow LUMO ($\lambda = 292$ nm, $f = 0.79$) as well as the other transitions and

leads to conclusion, that the molecule **6a** is presented at excitation as one complex chromophore system. For derivative **8b**, the most shifted maximum ($\lambda = 419$ nm, $f = 0.21$) is HOMO→LUMO transition again with HOMO orbital spreading over the whole molecular system. LUMO orbital however is limited really to acridine part of the molecule. Similar findings were assigned for other excitations, so we can conclude that in this case two chromophore systems are present.

Electron density can be reduced in the acridine moiety due to conjugation extending over the oxadiazole ring with the R group leading to diminished relative fluorescence. The changes in the fluorescence of compounds **8a–d** (see Table 1) due to the changing R substituent can be rationalized on the basis of electron withdrawal by the R group from the acridine segment via the oxadiazole ring. The more effective the electron withdrawal by the R group, the greater the reduction in fluorescence that can be expected. Electron withdrawal from the acridine segment is best facilitated by delocalization effected by conjugation and this process has been used previously to explain the fluorescence results observed in 9-iminoacridines.¹⁷ Thus, **8a** has the highest fluorescence of the set due to an electron-donating methyl group, but the fluorescence is reduced when the methyl is substituted by an electron withdrawing phenyl (**b**) or 3-pyridinyl (**c**) group. In the case of **d**, mesomeric structures can be drawn with a negative charge localized on nitrogen rather than on carbon, thus explaining the even further diminished relative fluorescence for this compound. Thus, **8a–d** follow an anticipated order: **b** and **c** have comparable fluorescence and are reduced with respect to **a**, whilst **d** has the least fluorescence of the set. In the case of **6a–e**, using **6a** (R = phenyl) as a base value, **6b–d** are all accordingly relatively more fluorescent since they all possess *para/ortho* directing groups in *para/ortho* positions on the attached phenyl group and

Table 1. Spectral characteristics for compounds **6a–e** and **8a–d**

Compound	Fluorescence ^a		
	λ_{\max} (nm)	F (a.u.)	F/F_0
6a	453	131.5	0.25
6b	448	237.9	0.44
6c	447	237.8	0.44
6d	448	212.5	0.40
6e	448	255.6	0.48
Acridone	448	534.8	1.00
8a	454	340.9	0.28
8b	453	223.9	0.18
8c	454	286.9	0.23
8d	454	104.3	0.08
Acridine-ITC	455	1237.0	1.00

^a Fluorescence emission spectra were recorded in the region 440–600 nm at an excitation wavelength of 412 nm for **6a–e** and 423 nm for **8a–d**. The relative fluorescence, F/F_0 , relates the fluorescence, F , of acridone at $\lambda_{\text{em}} = 448$ nm (concentration in methanol = 1.25×10^{-5} M) for **6a–e** and of acridine-ITC (acridine isothiocyanate) at $\lambda_{\text{em}} = 455$ nm (concentration in methanol = 1.08×10^{-5} M) for **8a–d**.

thus inhibit the additional flow of electrons from the acridone ring into the phenyl ring by conjugation, thereby leading to greater fluorescence. Inexplicably though, **6e** with a nitro group on the *meta* position of the attendant phenyl ring is the most fluorescent of the set and thus factors other than simple electron re-direction are in play in this case.

Molecular Modeling

Oxadiazoles **6a–e** were examined by quantum-chemical calculations using DFT at the B3LYP/6-311+G(d,p) level of theory and two low-energy rotamers for rotation about the C₂–C₄ bond were found as optimized structures (see Figure 4). Interestingly, the structural segments in both rotamers A and B are all coplanar, driven no doubt by a desire for extended delocalization, but also by the availability

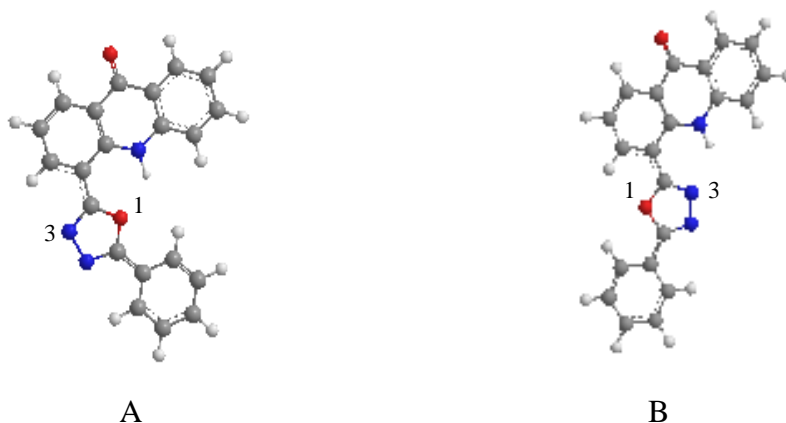


Figure 4. The two low energy rotamers for rotation about the C₂–C₄ bond found for compounds **6a–e** with either O-1 or N-3 of the oxadiazole ring proximal to H-10' (shown here for compound **6a**).

for intramolecular H-bonding between H-10' and the heteroatoms of the oxadiazole ring (O-1 or N-3). Similar coplanarity was also found for 2-oxadiazolo-5-yl aniline¹⁸ thus enabling efficient conjugation of the structural segments in that system and it is clear that the same stabilizing forces also drive this system here. Despite some predilection for steric hindrance due to the phenyl groups of the R substituent, in each case, the B rotamers, where N-3 is located close to H-10', were found to be lower in energy, ca. 6.5 kcal mol⁻¹, compared to structures A where O-1 is spatial to H-10'. This result may simply be just a reflection of the H-bonding preferences (sp³-hybridized O vs. sp²-hybridized N) as it does not appear that steric hindrance plays a role since **d**, with a sterically congestable 2,4,6-trimethylphenyl group, is not dissimilar to the other four members of the set. The calculated intramolecular distances $r_{O1,H10'}$ and $r_{N3,H10'}$ for A and B are very similar (1.974 and 1.934 Å, respectively). However, it is conceivable that the electron lone pairs of the oxygen in **6a–e** are weakened by conjugation with the ring nitrogen atoms. This is evident by the rather surprisingly low negative charge on the oxygen atom, particularly in comparison to the nitrogen

N-3 atom (Table 2). Moreover, in comparison between structures A and B, the charge on O-1 is little changed, since it is either H-bonding to H-10' (in structure A) or donating electrons to N-3 when it is not (structure B).

The charge on N-10' changes only modestly between the two structures, since H-bonding is present in both and it is only the donor atom that changes. For N-3, a sizeable change is observed between the two structures and this accounted for by greater electron donation from O-1 when it is not involved in H-bonding which renders it much more negative in structure B. Experimental findings from IR spectra (Figure 1) pointing out the presence both rotamers [N10-H...O (oxadiazol) and N10-H...N3 (oxadiazol)] are in accord with theoretical analysis.

Table 2. Calculated atomic charges (Q) on O-1, N-3, and N-10' for structures A and B of **6a–e**

	aA	aB	bA	bB	cA	cB	dA	dB	eA	eB
Q_{O}	-0.06	-0.03	-0.06	-0.02	-0.08	-0.03	-0.03	-0.08	-0.06	-0.02
Q_{N_3}	-0.09	-0.59	-0.04	-0.63	-0.12	-0.56	-0.14	-0.39	-0.06	-0.58
$Q_{\text{N}_{10'}}$	+0.32	+0.39	+0.31	+0.39	+0.32	+0.39	+0.32	+0.39	+0.32	+0.38

Oxadiazoles **8a–d** were also evaluated by quantum-chemical calculations at the same level of theory for two tautomers, H-11' and H-10'. The optimized tautomer structures are depicted in Figure 5 where the H-10' tautomers are seen to be able to maintain all three structural segments co-planar for conjugation despite obvious steric hindrance between the oxadiazole ring and H-8'. In the H-11' tautomers, this steric congestion is relieved by bond rotation about the N₁₁–C₉' bond as conjugation is less amenable through the sp³-hybridized N-11' thereby diminishing stabilization via this process.

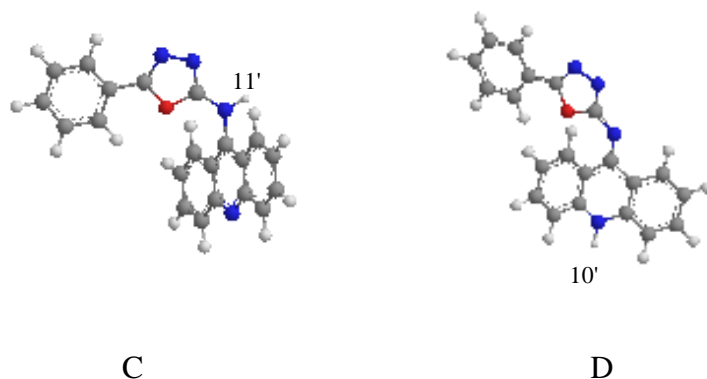


Figure 5. The H-11' tautomers (C) and H-10' tautomers (D) investigated for compounds **8a–d** (shown here for compound **8b**).

The H-10' tautomers (D), in concert with the spectroscopic results, were found to be preferred over their

H-11' tautomers (C) in each case, but moreover, there was a clear trend across the series (for **a** (CH₃), 1.8; **b** (phenyl), 2.1; **c** (3-pyridinyl), 2.6; and **d** (4-pyridinyl), 3.7 kcal mol⁻¹) indicating that the more effective the R substituent is in electron withdrawal, the more stable the H-10' tautomer is with respect to its counterpart H-11' tautomer. Only for the H-10' tautomer where N-11' is sp²-hybridized and able to conjugate can electron withdrawal by the R substituent proficiently stabilize the acridine ring. The importance of electron withdrawal as the stabilizing factor is clearly seen in the comparison of **c** and **d** where the *para* positioning of the ring nitrogen in **d** is better able to effect withdrawal (by supporting a negative charge in one mesomeric structure) in comparison to the *meta* positioned **c**: the H-10' tautomer of **d** is 1.25 kcal mol⁻¹ more stable than the H-10' tautomer of **c** but the H-11' tautomer of **d** is only 0.12 kcal mol⁻¹ more stable than the H-11' tautomer of **c**. Hence virtually all of the additional tautomeric stabilization of **d** emanates from its H-10' tautomer. Of significance, the tautomeric stability order of **a** < **b** < **c** < **d** reflects the afore described fluorescence order well with only **b** and **c** interchanged within the order. This is considered a correlation of some note and could be useful for adequately evaluating appropriate systems rapidly with regards to their potential applications, e.g. as fluorescence probes. Finally, calculation of the ¹³C NMR chemical shifts using the GIAO method at the DFT B3LYP/6-311++G(2d,2p) level of theory yielded a significant linear correlation when plotted against the experimental values for compounds **6a–e** (linear equation: $\delta_{\text{exp}} = 0.95 \times \delta_{\text{calc}} + 1.24$, correlation coefficient $r = 0.986$) and **8a–d** (linear equation: $\delta_{\text{exp}} = 0.98 \times \delta_{\text{calc}} - 1.98$, correlation coefficient $r = 0.987$), thereby substantiating the correctness of the assigned structures.

DNA binding properties

To evaluate the potential applications of **6c–e** as biological probes and/or potential drug therapeutic agents based on their intercalating properties, we investigated their binding efficiency and chromophore

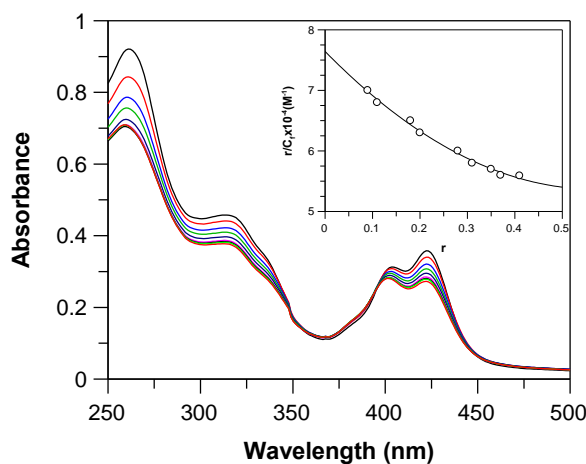


Figure 6. The changes in the UV-vis spectra of **6c** (40 μM in 10 mM Tris buffer, pH 7.3, 24 $^{\circ}\text{C}$) with increasing concentration of ctDNA. From top to bottom, 0–80 μM . Inset: Scatchard plot of **6c** complexation.

selective interactions with ctDNA using spectroscopic techniques. The UV-vis spectra of compounds **6c–e** exhibited broad absorption bands in the region 375–475 nm, typical for transitions between the π -electronic energy levels of the acridine skeleton. Upon the addition of ctDNA to the solutions of **6c–e**, a reduction in the absorbance by 28–33% from its initial value was observed which was dependent on the concentration of ctDNA. Figure 6 depicts these changes in the absorption spectra of **6c** upon increasing concentrations of ctDNA.

The DNA binding constants K of **6c–e** (Table 3) were determined using UV-vis titration according to the method of McGhee and von Hippel.¹⁹ Binding constants were found to be in the range $5.3–9.2 \times 10^4 \text{ M}^{-1}$

Table 3. DNA binding properties of derivatives **6c–e**

Compound	λ_{max} (nm)	Hypochromicity (%)	$K \times 10^4$ (M^{-1})	n
6a	414	<i>nd</i>	<i>nd</i>	<i>nd</i>
6b	422	<i>nd</i>	<i>nd</i>	<i>nd</i>
6c	423	25	7.8	2.6
6d	417	33	9.2	2.1
6e	420	28	5.3	3.4

nd – not determined

and the binding affinity values of compounds **6c–e** with ctDNA were found to be similar to values for proflavine–dithiazolidinone derivatives which have been reported recently.²⁰ The binding isotherms in each case were non-linear and concave upward, suggesting the involvement of more than one binding site. With multiple site binding (n lies in the range 2.1–3.4), the occurrence of one binding event is able to influence the interaction at neighboring sites. Binding constants and neighbor exclusion parameters clearly indicate a direct dependence between the intercalation capability and resulting structural changes in DNA binding. Upon the addition of ctDNA, the fluorescence properties of compounds **6c–e** was also affected with a resulting decrease in their fluorescence. Similar biological testing of oxadiazoles **8a–d** was precluded due to the decomposition of these compounds under Tris buffer conditions.

EXPERIMENTAL

Melting points were determined on a Boetius block and are uncorrected. NMR spectra were obtained at room temperature in hexadeuteriodimethyl sulfoxide ($\text{DMSO-}d_6$) using a Varian Mercury Plus NMR spectrometer operating at 400 MHz for ^1H and 100 MHz for ^{13}C . Tetramethylsilane was used as an internal standard for both ^1H and ^{13}C nuclei ($\delta_{\text{TMS}} = 0.00$ ppm for both). Heteronuclear HSQC and HMBC 2D experiments were optimized to 145 Hz (one-bond) and 8 Hz (long-range) for $J_{\text{H,C}}$ couplings. Elemental analyses were performed using a Perkin–Elmer CHN 2400 analyzer. IR spectra were recorded on a Nicolet 6700 FT IR instrument (samples in CS_2 solution, due to consistency with previous

azomethines¹¹). UV-vis spectra were measured on a Varian Cary 100 UV-vis spectrophotometer in methanol whilst the UV-vis titrations were conducted in 10 mM Tris buffer at pH 7.3. The concentration of compounds **6a–e** was 2.60×10^{-5} M and **8a–d** was 2.17×10^{-5} M. Fluorescence measurements were made using a Varian Cary Eclipse spectrofluorometer with a slit width of 10 nm for the excitation and emission beams in methanol. The concentration of **6a–e** was 1.25×10^{-5} M and that of **8a–d** was 1.08×10^{-5} M. Fluorescence intensities are expressed in arbitrary units. The concentration of ctDNA (purchased from Sigma Chemical Co.) was varied over the range 0–80 μ M. All measurements were performed at 24 °C. The absorption data were used to construct binding plots according to the method of McGhee and von Hippel using data points from a Scatchard plot.^{20,21} The binding data were fitted using GNU Octave 2.1.73 software. DFT quantum-chemical calculations were performed using the *Gaussian 03* program at the B3LYP/6-311+G(d,p) level of theory.^{22,23} The GIAO method²⁴ was used to obtain ¹³C NMR chemical shifts with the 6-311++G(2d,2p) basis set. UV-vis spectral analysis was carried out using ZINDO method.²⁵

General procedure for the preparation of hydrazide 4

To an ethanolic solution of hydrazine monohydrate (0.82 mL, 15.85 mmol) an ethanolic solution of ester **3** (1 g, 3.95 mmol) was added. The reaction mixture was refluxed until the formation of a precipitant (ca. 4 h). The reaction mixture was then cooled and the precipitant filtered off and dried. Yield 80%; mp 314–316 °C; ¹H NMR (400 MHz, DMSO-*d*₆) δ : 4.72 (bs, 2H, NH₂), 7.30–7.35 (m, 2H, H-2,7), 7.71–7.79 (m, 2H, H-5,6), 8.16 (dd, 1H, H-3, *J* = 8.4, 1.4 Hz), 8.24 (dd, 1H, H-8, *J* = 8.4, 1.2 Hz), 8.43 (dd, 1H, H-1, *J* = 9.6, 1.4 Hz), 10.26 (s, 1H, NH), 12.28 (s, 1H, H-10); ¹³C NMR (100 MHz, DMSO-*d*₆) δ : 117.8 (C-4), 118.2 (C-5), 120.0 (C-2), 120.3 (C-9a), 121.42 (C-8a), 121.8 (C-7), 125.8 (C-8), 129.7 (C-1), 132.3 (C-3), 133.9 (C-6), 139.9 (C-4a), 139.9 (C-10a), 166.6 (C=O), 176.45 (C-9); Anal. Calcd for C₁₄H₁₁N₃O₂ (253.26): C, 66.40; H, 4.38; N, 16.59. Found: C, 66.95; H, 4.17; N, 16.23%.

Aldimines **5a–e** were prepared according to the procedure described previously.¹¹

General procedure for the preparation of oxadiazoles 6a–e

To a mixture of aldimine (0.26 mmol) and anhydrous sodium acetate (0.26 mmol) in glacial acetic acid bromine in glacial acetic acid (0.26 mmol) was added. The reaction mixture was stirred at rt for 2 h followed by the addition of acetic anhydride (1 mL) after which the reaction mixture was left to stir for 24 h at 100 °C. The reaction mixture was then dried under reduced pressure and extracted into CHCl₃ following which the solvent was removed and the crude product recrystallized from MeOH.

4-(5-Phenyl[1,3,4]oxadiazol-2-yl)-10H-acridin-9-one (6a). Yield 65%; mp 227–230 °C; IR (CS₂, hydrogen bondings) 3441.0 and 3443.2 cm⁻¹; UV-vis $\lambda = 411$ nm (log $\epsilon = 3.67$), $\lambda = 299$ nm (log $\epsilon = 3.79$); ¹H NMR (CDCl₃) δ : 7.30 (t, 1H, H-7', $J = 8.0$ Hz), 7.36 (t, 1H, H-2', $J = 7.6$ Hz), 7.50 (d, 1H, H-5', $J = 8.4$ Hz), 7.58–7.62 (m, 3H, H-3'',4'',5''), 7.69 (m, 1H, H-6'), 8.17 (dd, 2H, H-2'',6'', $J = 7.6, 1.6$ Hz), 8.34 (d, 1H, H-3', $J = 7.2$ Hz), 8.44 (d, 1H, H-8', $J = 7.6$ Hz), 8.67 (d, 1H, H-1', $J = 7.6$ Hz), 11.81 (s, 1H, H-10'); ¹³C NMR (CDCl₃) δ : 109.1 (C-4'), 117.7 (C-5'), 120.4 (C-2'), 121.6 (C-8a'), 122.4 (C-9a'), 122.6 (C-7'), 123.1 (C-1''), 127.0 (C-8'), 127.1 (C-3'',5''), 129.3 (2'',6''), 131.9 (C-1'), 132.3 (C-3'), 132.3 (C-4''), 134.1 (C-6'), 138.7 (C-4a'), 140.3 (C-10a'), 163.4 (C-2), 163.6 (C-5), 177.8 (C-9'). Anal. Calcd for C₂₁H₁₃N₃O₂ (339.36): C, 74.33; H, 3.86; N, 12.38. Found: C, 74.12; H, 3.78; N, 12.01%.

4-[5-(4-Bromophenyl)-[1,3,4]oxadiazol-2-yl]-10H-acridin-9-one (6b). Yield 37%; mp 229–232 °C; UV-vis $\lambda = 413$ nm (log $\epsilon = 4.18$), $\lambda = 390$ nm (log $\epsilon = 3.99$), $\lambda = 320$ nm (log $\epsilon = 4.23$), $\lambda = 298$ nm (log $\epsilon = 4.21$); ¹H NMR (CDCl₃) δ : 7.35–7.30 (m, 2H, H-2',7'), 7.42 (d, 2H, H-2'',6'', $J = 8.4$ Hz), 7.57 (d, 2H, H-3'',5'', $J = 8.8$ Hz), 7.78–7.70 (m, 2H, H-5',6'), 8.16 (d, 1H, H-3', $J = 7.6$ Hz), 8.47 (d, 1H, H-8', $J = 8.4$ Hz), 8.67 (d, 1H, H-1', $J = 8.0$ Hz), 11.04 (s, 1H, H-10'); ¹³C NMR (CDCl₃) δ : 109.2 (C-4'), 117.2 (C-5'), 120.5 (C-2'), 121.7 (C-9a'), 122.1 (C-8a'), 122.8 (C-4''), 122.8 (C-7'), 124.6 (C-1''), 127.3 (C-8'), 128.3 (C-2'',6''), 132.1 (C-1'), 132.2 (C-3'',5''), 133.5 (C-3'), 134.1 (C-6'), 138.7 (C-4a'), 139.9 (C-10a'), 155.1 (C-5), 167.3 (C-2), 177.7 (C-9'). Anal. Calcd for C₂₁H₁₂BrN₃O₂ (418.25): C, 60.31; H, 2.89; N, 10.05. Found: C, 60.48; H, 2.85; N, 9.97%.

4-[5-(4-Methoxyphenyl)-[1,3,4]oxadiazol-2-yl]-10H-acridin-9-one (6c). Yield 40%; mp 226–228 °C; UV-vis $\lambda = 412$ nm (log $\epsilon = 4.28$), $\lambda = 392$ nm (log $\epsilon = 4.14$), $\lambda = 322$ nm (log $\epsilon = 4.31$), $\lambda = 311$ nm (log $\epsilon = 4.37$); ¹H NMR (CDCl₃) δ : 3.92 (s, 3H, OCH₃), 7.07 (m, 2H, H-3'',5''), 7.32 (t, 1H, H-7', $J = 7.4$ Hz), 7.38 (t, 1H, H-2', $J = 7.6$ Hz), 7.52 (d, 1H, H-5', $J = 8.4$ Hz), 7.71 (t, 1H, H-6', $J = 7.8$ Hz), 8.11 (d, 2H, H-2'',6'', $J = 9.2$ Hz), 8.35 (dd, 1H, H-3', $J = 7.2, 1.6$ Hz), 8.46 (dd, 1H, H-8', $J = 8.4, 1.6$ Hz), 8.69 (dd, 1H, H-1', $J = 8.4, 1.6$ Hz), 11.87 (s, 1H, H-10'); ¹³C NMR (CDCl₃) δ : 55.6 (OCH₃), 109.4 (C-4'), 114.7 (C-3'',5''), 115.5 (C-1''), 117.8 (C-5'), 120.4 (C-2'), 121.7 (C-8a'), 122.4 (C-9a'), 122.6 (C-7'), 127.1 (C-8'), 128.9 (C-2'',6''), 131.7 (C-1'), 132.2 (C-3'), 134.1 (C-6'), 138.7 (C-4a'), 140.4 (C-10a'), 162.9 (C-4''), 163.0 (C-2), 163.7 (C-5), 177.9 (C-9'). Anal. Calcd for C₂₂H₁₅N₃O₃ (369.38): C, 71.54; H, 4.09; N, 11.38. Found: C, 71.08; H, 3.96; N, 11.02%.

4-[5-(2,4,6-Trimethylphenyl)-[1,3,4]oxadiazol-2-yl]-10H-acridin-9-one (6d). Yield 72%; mp 216–218 °C; IR (CS₂, hydrogen bondings) 3414.7 and 3444.7 cm⁻¹; UV-vis $\lambda = 411$ nm (log $\epsilon = 4.07$), $\lambda = 391$ nm

(log $\epsilon = 3.93$), $\lambda = 326$ nm (log $\epsilon = 3.20$), $\lambda = 305$ nm (log $\epsilon = 4.02$); ^1H NMR (CDCl_3) δ : 2.38 (s, 3H, H-4'''), 2.39 (s, 6H, H-2''',6'''), 7.04 (s, 2H, H-3'',5''), 7.32–7.37 (m, 2H, H-2',7'), 7.56 (d, 1H, H-5', $J = 8.0$ Hz), 7.73 (m, 1H, H-6'), 8.30 (dd, 1H, H-3', $J = 7.2, 1.4$ Hz), 8.47 (dd, 1H, H-8', $J = 8.0, 1.6$ Hz), 8.70 (dd, 1H, H-1', $J = 7.6, 1.4$ Hz), 11.93 (s, 1H, H-10'); ^{13}C NMR (CDCl_3) δ : 20.7 (C-2''',6'''), 21.4 (C-4'''), 109.4 (C-4'), 117.8 (C-5'), 120.2 (C-1''), 120.5 (C-2'), 121.7 (C-8a'), 122.4 (C-9a'), 122.6 (C-7'), 127.1 (C-8'), 129.2 (C-3'',5''), 131.9 (C-1'), 132.4 (C-3'), 134.1 (C-6'), 138.8 (C-4a'), 138.9 (C-2'',6''), 140.4 (C-10a'), 141.7 (C-4''), 163.2 (C-5), 163.8 (C-2), 177.9 (C-9'). Anal. Calcd for $\text{C}_{24}\text{H}_{19}\text{N}_3\text{O}_2$ (381.44): C, 75.57; H, 5.02; N, 11.02. Found: C, 75.16; H, 4.91; N, 10.86%.

4-[5-(3-Nitrophenyl)-[1,3,4]oxadiazol-2-yl]-10H-acridin-9-one (*6e*). Yield 68%; mp 267–269 °C; IR (CS_2 , hydrogen bondings) 3413.6 and 3443.3 cm^{-1} ; UV-vis $\lambda = 412$ nm (log $\epsilon = 4.23$), $\lambda = 390$ nm (log $\epsilon = 4.07$), $\lambda = 297$ nm (log $\epsilon = 4.17$); ^1H NMR (CDCl_3) δ : 7.23 (s, 1H, H-2''), 7.31–7.34 (m, 2H, H-2',7'), 7.66 (t, 1H, H-5'', $J = 8.4$ Hz), 7.73 (t, 1H, H-6', $J = 7.6$ Hz), 7.94 (d, 1H, H-4'', $J = 8.4$ Hz), 8.17 (dd, 1H, H-3', $J = 7.2, 1.2$ Hz), 8.32 (m, 1H, H-6''), 8.40 (m, 1H, H-5'), 8.48 (dd, 1H, H-8', $J = 8.0, 1.2$ Hz), 8.69 (dd, 1H, H-1', $J = 7.2, 1.2$ Hz), 10.98 (s, 1H, H-10''); ^{13}C NMR (CDCl_3) 108.9 (C-4'), 117.2 (C-2''), 120.6 (C-2'), 121.0 (C-1''), 121.7 (C-9a'), 121.8 (C-5'), 122.2 (C-8a'), 122.9 (C-7'), 125.2 (C-6''), 127.4 (C-8'), 130.2 (C-5''), 132.4 (C-1'), 132.9 (C-4''), 133.5 (C-3'), 134.2 (C-6'), 137.7 (C-3''), 138.8 (C-4a'), 139.9 (C-10a'), 155.1 (C-5), 167.7 (C-2), 177.7 (C-9'). Anal. Calcd for $\text{C}_{21}\text{H}_{12}\text{N}_4\text{O}_4$ (384.35): C, 65.63; H, 3.15; N, 14.58. Found: C, 65.21; H, 3.07; N, 14.25%.

General procedure for the synthesis of 1,3,4-oxadiazoles **8a–d**

Method A: To a boiling solution of acylthiosemicarbazides **7a–d**^{9b} (0.4 mmol) in absolute EtOH (4 mL), finely powdered mercuric oxide (0.9 mmol) was added portion-wise over a period of 30 min. The resulting suspension was heated under reflux for 2 h and then filtered whilst hot. The black precipitate was washed with boiling EtOH (3 \times 3 mL) and the combined filtrate and washings were concentrated to a small volume and set aside overnight at rt. The separated product was filtered, dried and recrystallized from MeOH.

Method B: A mixture of acylsemicarbazide (0.27 mmol) and POCl_3 (0.95 mL) was heated on an oil bath until the reaction was complete (monitored by TLC, CHCl_3 –MeOH, 9:1). The reaction mixture was cooled to rt, diluted with CH_2Cl_2 (8 mL) and then poured into 25 mL of an ice–water mixture with stirring. After cooling to rt and extraction with a mixture of CH_2Cl_2 –MeOH (1:1), the combined organic extracts were washed with H_2O , brine, and then dried over MgSO_4 . The solvent was evaporated in vacuo and the residue purified by flash chromatography (silica gel, CHCl_3 –MeOH).

(10*H*-Acridin-9-ylidene)-(5-methyl[1,3,4]oxadiazol-2-yl)amine (8a). Yield 13%; mp 222–224 °C; UV-vis $\lambda = 423$ nm (log $\epsilon = 4.13$), $\lambda = 394$ nm (log $\epsilon = 3.89$), $\lambda = 265$ nm (log $\epsilon = 4.45$); ^1H NMR (DMSO- d_6) δ : 2.42 (s, 3H, CH₃), 7.22 (dd, 2H, H-2',7', $J = 8.0, 7.0$ Hz), 7.58 (d, 2H, H-4',5', $J = 8.4$ Hz), 7.73 (dd, 2H, H-3',6', $J = 8.4, 7.0$ Hz), 7.90 (d, 2H, H-1',8', $J = 8.0$ Hz), 12.09 (s, 1H, NH); ^{13}C NMR (DMSO- d_6) δ : 11.0 (CH₃), 117.1 (C-8a',9a'), 117.7 (C-4',5'), 121.7 (C-2',7'), 126.4 (C-1',8'), 133.4 (C-3',6'), 139.7 (C-4a',10a'), 159.7 (C-5), 159.8 (C-9'), 166.1 (C-2). Anal. Calcd for C₁₆H₁₂N₄O (276.30): C, 69.55; H, 4.38; N, 20.28. Found: C, 69.28; H, 4.17; N, 20.03%.

(10*H*-Acridin-9-ylidene)-(5-phenyl[1,3,4]oxadiazol-2-yl)amine (8b). Yield 12%; mp 297–300 °C; UV-vis $\lambda = 419$ nm (log $\epsilon = 4.04$), $\lambda = 389$ nm (log $\epsilon = 3.86$); ^1H NMR (DMSO- d_6) δ : 7.25 (ddd, 2H, H-2',7', $J = 8.2, 7.0, 1.2$ Hz), 7.50–7.60 (m, 3H, H-2'',4'',6''), 7.63 (dd, 2H, H-4',5', $J = 8.2, 1.2$ Hz), 7.77 (ddd, 2H, H-3',6', $J = 8.2, 7.0, 1.2$ Hz), 7.85–7.95 (m, 2H, H-3'',5''), 8.01 (dd, 2H, H-1',8', $J = 8.2, 1.2$ Hz), 12.28 (s, 1H, NH); ^{13}C NMR (DMSO- d_6) δ : 117.6 (C-8a',9a'), 118.3 (C-4',5'), 122.4 (C-2',7'), 124.8 (C-1''), 126.0 (C-3'',5''), 126.9 (C-1',8'), 129.8 (C-2'',6''), 131.4 (C-4''), 134.1 (C-3',6'), 140.2 (C-4a',10a'), 160.7, 160.8 (C-5, C-9'), 166.6 (C-2); Anal. Calcd for C₂₁H₁₄N₄O (338.37): C, 74.54; H, 4.17; N, 16.56. Found: C, 74.26; H, 3.98; N, 16.37%.

(10*H*-Acridin-9-ylidene)-(5-pyridin-3-yl[1,3,4]oxadiazol-2-yl)amine (8c). Yield 15%; mp 292–294 °C; UV-vis $\lambda = 427$ nm (log $\epsilon = 3.99$), $\lambda = 400$ nm (log $\epsilon = 3.78$), $\lambda = 269$ nm (log $\epsilon = 4.33$); ^1H NMR (DMSO- d_6) δ : 7.26 (dd, 2H, H-2',7', $J = 8.0, 7.2$ Hz), 7.59 (dd, 1H, H-5'', $J = 8.0, 4.8$ Hz), 7.65 (d, 2H, H-4',5', $J = 8.0$ Hz), 7.78 (ddd, 2H, H-3',6', $J = 8.0, 7.2, 1.2$ Hz), 8.05 (dd, 2H, H-1',8', $J = 8.0, 1.2$ Hz), 8.27 (ddd, 1H, H-4'', $J = 8.0, 2.0, 1.6$ Hz), 8.74 (dd, 1H, H-6'', $J = 4.8, 1.6$ Hz), 9.09 (d, 1H, H-2'', $J = 2.0$ Hz), 12.35 (s, 1H, NH); ^{13}C NMR (DMSO- d_6) δ : 117.0 (C-8a',9a'), 117.8 (C-4',5'), 120.8 (C-3''), 121.9 (C-2',7'), 124.2 (C-5''), 126.4 (C-1',8'), 132.9 (C-4''), 133.6 (C-3',6'), 139.7 (C-4a',10a'), 146.2 (C-2''), 151.3 (C-6''), 158.3 (C-5), 160.4 (C-9'), 166.4 (C-2); Anal. Calcd for C₂₀H₁₃N₅O (339.36): C, 70.79; H, 3.86; N, 20.64. Found: C, 70.54; H, 3.69; N, 20.41%.

(10*H*-Acridin-9-ylidene)-(5-pyridin-4-yl[1,3,4]oxadiazol-2-yl)amine (8d). Yield 12%; mp 324–326 °C; UV-vis $\lambda = 429$ nm (log $\epsilon = 3.74$), $\lambda = 390$ nm (log $\epsilon = 3.53$); ^1H NMR (DMSO- d_6) δ : 7.27 (dd, 2H, H-2',7', $J = 8.0, 7.2$ Hz), 7.66 (d, 2H, H-4',5', $J = 8.4$ Hz), 7.70–7.90 (m, 4H, H-3',6',3'',5''), 8.04 (d, 2H, H-1',8', $J = 8.0$ Hz), 8.76 (m, 2H, H-2'',6''), 12.41 (s, 1H, NH); ^{13}C NMR (DMSO- d_6) δ : 117.5 (C-8a',9a'), 118.4 (C-4',5'), 119.7 (C-3'',5''), 122.6 (C-2',7'), 126.9 (C-1',8'), 131.7 (C-4''), 134.3 (C-3',6'), 140.2 (C-4a',10a'), 151.2 (C-2'',6''), 159.0 (C-5), 161.1 (C-9'), 167.3 (C-2); Anal. Calcd For C₂₀H₁₃N₅O

(339.36): C, 70.79; H, 3.86; N, 20.64. Found: C, 70.47; H, 3.62; N, 20.45%.

4-(9,10-Dihydroacridin-9-ylidene)-1-(4-pyridinylcarbonyl)semicarbazide (9d). To a solution of acylthiosemicarbazide **7d** (0.40 mmol) in MeCN (2 mL), MNO (0.49 mmol) was added and the reaction mixture stirred at rt until the reactants had been consumed (monitored by TLC, CHCl₃–MeOH, 9:1). The precipitate that formed was filtered off, washed with MeCN and dried at rt. The crude product was recrystallized from MeOH. Yield 95%; mp 154–156 °C; ¹H NMR (DMSO-*d*₆) δ: 7.17 (dd, 1H, H-2', *J* = 8.0, 7.4 Hz), 7.43 (d, 1H, H-4', *J* = 8.0 Hz), 7.64 (dd, 2H, H-3',6', *J* = 8.0, 7.4 Hz), 7.80–8.00 (m, 3H, H-3'',5'',7''), 8.16 (d, 1H, H-8', *J* = 8.0 Hz), 8.25 (d, 1H, H-5', *J* = 8.0 Hz), 8.40 (d, 1H, H-1', *J* = 8.0 Hz), 8.75–8.85 (m, 2H, H-2'',6''), 9.52 (s, 1H, NH), 10.64 (s, 1H, NH), 11.44 (s, 1H, H-10'); ¹³C NMR (DMSO-*d*₆) δ: 117.3 (C-4'), 117.6 (C-8a'), 121.4 (C-2'), 121.9 (C-3'',5''), 122.1 (C-9a'), 125.2 (C-5'), 126.0, 133.0 (C-3', C-6'), 128.0 (C-1'), 129.6 (C-8), 130.8 (C-7'), 140.1, 140.4 (C-4a', C-4''), 149.4 (C-10a'), 150.8 (C-2'',6''), 154.3 (C-9'), 164.3 (C-3), 165.4 (Py–C=O); Anal. Calcd For C₂₀H₁₅N₅O₂ (357.37): C, 67.22; H, 4.23; N, 19.60. Found: C, 66.97; H, 4.06; N, 19.33%.

ACKNOWLEDGEMENTS

Financial support for this work from the Slovak Grant Agency VEGA (grants no. 1/0476/08, 1/0053/08), the State NMR Program (grant no. 2003SP200280203), and Turun Yliopistosäätiö is gratefully acknowledged.

REFERENCES

1. S. A. F. Rostom, M. A. Shalaby, and M. A. El-Demellawy, *Eur. J. Med. Chem.*, 2003, **38**, 959.
2. Ş. G. Küçükgülzel, E. E. Oruç, S. Rollas, F. Ş. Sahin, and A. Özbek, *Eur. J. Med. Chem.*, 2002, **37**, 197.
3. P. Mishra, H. Rajak, and A. Mehta, *J. Gen. Appl. Microbiol.*, 2005, **51**, 133.
4. K. M. Khan, Zia-Ullah, M. Rani, S. Perveen, S. M. Haider, M. I. Choudhary, Atta-ur-Rahman, and W. Voelter, *Lett. Org. Chem.*, 2004, **1**, 50.
5. I. R. Baxendale, S. V. Ley, and M. Martinelli, *Tetrahedron*, 2005, **61**, 5323 and references cited therein.
6. M. A. M. Taha and S. M. El-Badry, *J. Chin. Chem. Soc.*, 2006, **53**, 1181 and references cited therein.
7. G. S. Poindexter, M. A. Bruce, J. G. Breitenbucher, M. A. Higgins, S.-Y. Sit, J. L. Romine, S. W. Martin, S. A. Ward, R. T. McGovern, W. Clarke, J. Russell, and I. Antal-Zimanyi, *Bioorg. Med. Chem.*, 2004, **12**, 507.

8. W. Ogilvie and W. Rank, [Can. J. Chem.](#), 1987, **65**, 166.
9. a) D. Sabolová, M. Kožurková, P. Kristian, I. Danihel, D. Podhradský, and J. Imrich, [Int. J. Biol. Macromol.](#), 2006, **38**, 94. b) J. Tomaščíková, J. Imrich, I. Danihel, S. Böhm, P. Kristian, J. Pisarčíková, M. Sabol, and K. D. Klika, [Molecules](#), 2008, **13**, 501. c) M. Kožurková, D. Sabolová, H. Paulíková, L. Janovec, P. Kristian, M. Bajdichová, J. Buša, D. Podhradský, and J. Imrich, [Int. J. Biol. Macromol.](#), 2007, **41**, 415. d) M. Kožurková, D. Sabolová, L. Janovec, J. Mikeš, J. Kovař, J. Ungvarský, M. Štefanišinová, P. Fedoročko, P. Kristian, and J. Imrich, [Bioorg. Med. Chem.](#), 2008, **16**, 3976. e) Z. Gažová, A. Bellová, Z. Daxnerová, J. Imrich, P. Kristian, J. Tomaščíková, J. Bágel'ová, D. Fedunová, and M. Antalík, [Eur. Biophys. J.](#), 2008, **37**, 1261. f) S. Hamuřáková, P. Kristian, D. Jun, K. Kuča, J. Imrich, I. Danihel, S. Böhm, and K. D. Klika, [Heterocycles](#), 2008, **76**, 1219.
10. V. Sourdou, S. Mazoyer, V. Pique, and J.-P. Galay, [Molecules](#), 2001, **6**, 673.
11. Z. Fröhlichová, J. Imrich, I. Danihel, P. Kristian, S. Böhm, D. Sabolová, O. Hritzová, B. Horváth, T. Bušová and K. D. Klika, submitted to *Spectroc. Acta Pt. A*, 2008.
12. Z. Shang, [Synthetic Commun.](#), 2006, **36**, 2927.
13. M. Dabiri, P. Salehi, M. Baghbanzadeh, and M. Bahramnejad, [Tetrahedron Lett.](#), 2006, **47**, 6983.
14. F. N. Hayes, B. S. Rogers, and D. G. Ott, [J. Am. Chem. Soc.](#), 1955, **77**, 1850.
15. D. R. Romer, R. B. Shankar, and R. G. Pews, PCT/US 1995/013493.
16. a) K. D. Klika, E. Balentová, J. Bernát, J. Imrich, M. Vavrušová, E. Kleinpeter, K. Pihlaja, and A. Koch, [J. Heterocycl. Chem.](#), 2006, **43**, 633. b) E. Balentová, J. Imrich, J. Bernát, L. Suchá, M. Vilková, N. Prónayová, P. Kristian, K. Pihlaja, and K. D. Klika, [J. Heterocycl. Chem.](#), 2006, **43**, 645. c) K. D. Klika, E. Balentová, J. Bernát, J. Imrich, M. Vavrušová, K. Pihlaja, A. Koch, E. Kleinpeter, A. Kelling, and U. Schilde, [ARKIVOC](#), 2006, (xvi), 93. d) J. Bernát, E. Balentová, P. Kristian, J. Imrich, E. Sedlák, I. Danihel, S. Böhm, N. Prónayová, K. Pihlaja, and K. D. Klika, [Coll. Czech. Chem. Commun.](#), 2004, **69**, 833. e) K. D. Klika, J. Imrich, M. Vilková, J. Bernát, and K. Pihlaja, [J. Heterocycl. Chem.](#), 2006, **43**, 739. f) K. D. Klika, J. Bernát, J. Imrich, I. Chomča, R. Sillanpää, and K. Pihlaja, [J. Org. Chem.](#), 2001, **66**, 4416. g) P. Kristian, E. Balentová, J. Bernát, J. Imrich, E. Sedlák, I. Danihel, S. Böhm, N. Prónayová, K. D. Klika, K. Pihlaja, and J. Baranová, [Chem. Pap.](#), 2004, **58**, 268. h) B. Adcock, 'Aminoacridines' In 'Acridines', ed. by R. M. Acheson, (from 'The Chemistry of Heterocyclic Compounds' ed. by A. Weissberger and E. C. Taylor), J. Wiley: New York, 1973, p. 109.
17. P. Kristian, J. Bernát, J. Imrich, E. Sedlák, J. Alföldi, and M. Čornanič, [Heterocycles](#), 2001, **55**, 279.
18. A. Souldozi, K. Slepokura, T. Lis, and A. Ramazani, [Z. Naturforsch. \(B\)](#), 2007, **62**, 835.
19. J. McGhee and P. von Hippel, [J. Mol. Biol.](#), 1974, **86**, 469.

20. L. Janovec, D. Sabolová, M. Kožurková, H. Paulíková, P. Kristian, J. Ungvarský, E. Moravčíková, M. Bajdichová, D. Podhradský, and J. Imrich, [Bioconjug. Chem., 2007, 18, 93](#).
21. T. C. Jenkins, *Methods in Molecular Biology*, K. R. Fox, Humana Press, Totowa, New Jersey, 1997, **90**, 195.
22. A. D. Becke, [J. Chem. Phys., 1993, 98, 5648](#).
23. M. J. Frisch, G. W. Trucks, H. B. Schlegel, G. E. Scuseria, M. A. Robb, J. R. Cheeseman, J. A. Montgomery Jr., T. Vreven, K. N. Kudin, J. C. Burant, J. M. Millam, S. S. Iyengar, J. Tomasi, V. Barone, B. Mennucci, M. Cossi, G. Scalmani, N. Rega, A. Petersson, H. Nakatsuji, M. Hada, M. Ehara, K. Toyota, R. Fukuda, J. Hagesawa, M. Ishida, T. Nakajima, Y. Honda, O. Kitao, H. Nakai, M. Klene, X. Li, J. E. Knox, H. P. Hratchian, J. B. Cross, C. Adamo, J. Jaramillo, R. Gomperts, E. Stratmann, O. Yazyev, A. J. Austin, R. Cammi, C. Pomelli, J. W. Ochterski, P. Y. Ayala, K. Morokuma, G. A. Voth, P. Salvador, J. J. Dannenberg, V. G. Zakrzewski, S. Dapprich, A. D. Daniels, M. C. Strain, O. Farkas, D. K. Malick, A. D. Rabuck, K. Raghavachari, J. B. Foresman, J. V. Ortiz, Q. Cui, A. G. Baboul, S. Clifford, J. Cioslowski, B. B. Stefanov, G. Liu, A. Liashenko, P. Piskorz, I. Komaromi, R. L. Martin, D. J. Fox, T. Keith, M. A. Al-Laham, C. Y. Peng, A. Nanayakkara, M. Challacombe, P. M. W. Gill, B. Johnson, W. Chen, M. W. Wong, C. Gonzales, and J. A. Pople, *Gaussian 03, Revision B.05*, Gaussian, Inc., Pittsburgh PA 2003.
24. K. Wolinski, J. F. Hinton, and P. Pulay, [J. Am. Chem. Soc., 1990, 112, 8251](#).
25. L. K. Hanson, J. Fajer, M. A. Thompson, and M. C. Zerner, [J. Am. Chem. Soc., 1987, 109, 4728](#).